RESEARCH PAPER

Dual-targeted drug delivery system based on dopamine functionalized human serum albumin nanoparticles as a carrier for methyltestosterone drug

Tayebeh Noori [1], Soheila Kashanian [2, 3], Ronak Rafipour [4], Kamran Mansouri [5], Maryam Nazari [1]*

[1]*Department of Applied Chemistry, Faculty of Chemistry, Razi University, Kermanshah, Iran*
[2]*Faculty of Chemistry, Sensor and Biosensor Research Center (SBRC) & Nanoscience and Nanotechnology Research Center (NNRC), Razi University, Kermanshah, Iran*
[3]*Nano Drug Delivery Research Center, Kermanshah University of Medical Sciences, Kermanshah, Iran*
[4]*Department of Chemistry, Kermanshah Branch, Islamic Azad University, Kermanshah, Iran*
[5]*Medical Biology Research Center (MBRC), Kermanshah University of Medical Sciences, Kermanshah, Iran*

ABSTRACT

Objective(s): This study aims to enhance 17 a-methyltestosterone loaded human serum albumin nanoparticles (MT-HSA NPs) bioavailability through a desolvation technique. Dopamine (DA) molecules were conjugated on the surface of MT-HSA NPs and have the potential to act as tiny proper ligands in a unique treatment system to cope with cancer in which drug will be transmitted to the cancer area. Herein, we used HSA as an adaptable carrier of anticancer agents for methyltestosterone transport to the tumor site via DA D1-D5 receptors. In the present study, sonication of MT-HSA solution was carried out before the desolvation procedure to increase the drug loading and entrapment efficiency.
Materials and Methods: Various parameters were optimized to characterize NPs including morphology, size, zeta potential, polydispersity index, drug release profile, and entrapment efficiency.
Results: Under the optimum conditions of HSA and drug (1:41), at pH 9, results demonstrate sizes of 69 nm and 82 nm for MT-HSA and MT-HSA-DA NPs respectively. For MT-HSA NPs, the polydispersity index was found to be 0.3 and the average drug loading and encapsulation efficiency were 14% and 91% respectively. Anticancer activity and the release of drug was investigated through MCF-7 breast cancer cell line. Results show that targeted NPs are more effective than non-targeted NPs.
Conclusion: According to these studies, the therapeutic effects against various diseases such as cancers increase through cellular targeting property of a biocompatible drug delivery system. This is the first report for methyltestosterone delivery to breast cancer cells based on HSA NPs.

Keywords: *Encapsulation, Drug delivery system, Targeting, 17α-methyltestosterone*

INTRODUCTION

To date, chemotherapy, radiation therapy, and surgical intervention or a combination of these options are applied to cancer treatment options [1]. However, disadvantages of these strategies such as low access to drugs at the tumor sites, renal toxicity, or hepatic toxicity lead to overcome their benefits. Recently, as an effective anticancer delivery system, nanoparticulate drug delivery systems (NDDS) have been established [2]. Their

tiny size, bioavailability, biodegradability, high drug loading, the long-term circuit in the blood, and the capacity to active or passive targeting of a determined area are desired properties of NDDS [3]. There are different types of drug delivery systems including polymeric micelles [4], liposomes [5], dendrimers [6], and drug conjugated polymers [7, 8]. There is a promotion in protein nanocarriers that are developing, in general, considered as protected drug delivery instruments because of their biodegradability, high dietetically value, non-antigenicity, the excellent binding capacity of different drugs and

abundant renewable sources [9].

Human serum albumin (HSA) is the most frequent substance in human blood plasma (almost about 35-50 g/L). The liver has to produce HSA with a 19-day half-life in the human body [10]. This protein with low tryptophan content and rich in cysteine is a single polypeptide with 585 amino acids. HSA with three structural domains (I, II, and III) can be observed using structural analysis of X-ray. Each domain is divided into two sub-domains that named "A" and "B" [11]. Albumin has a multi-functional ability and high binding capacity to deliver many fatty acids, hydrophilic and hydrophobic drugs, bilirubin, ions, and different hormones due to the different drug-binding sites in the molecular domains [12]. HSA nanoparticles (HSA-NPs) are formed by the assembly of HSA molecules in solution forming intermolecular disulfide bonds [13]. There are several different techniques to the production of albumin NPs that include coacervation, emulsion formation, and desolvation [14]. In the desolvation method reproducibility and controlled drug release is high compared to other techniques [15].

HSA can resist heat up to 60°C for 10 hours and is stable within the pH range of 4-9 [16]. Various anti-cancer drugs, such as paclitaxel [17] curcumin [18] docetaxel [19] and 5-fluorouracil [20] can deliver to cancer cell via the HSA glycoprotein 60 (GP60) receptor present on the surface of cancer cells, without causing an immune response, hence increase the bioavailability and distribution of the drug [13].

The dual-targeted delivery systems are developed to improve the selectivity of drugs to cancer cells [2]. To date, several ligand-receptor systems have been studied for targeted drug delivery.

In the field of targeted drug delivery, various ligand-receptor systems have been investigated such as lipoprotein receptors, transferrin receptors, lectin receptors, interleukin receptors, and receptors expressed on the cancer cells [21]. Dopamine (DA) receptors are an example of these receptors which are overexpressed in some of the cancer cells, such as human breast cancer and colon adenocarcinoma [22, 23]. Borcherding et al., indicated in breast cancer, DA type-1 receptors (D1R) expression identifying receptors as a novel therapeutic target. Signaling the cGMP-protein kinase (PKG) pathway through DA and D1R agonists, threat viability, and invasion of the cell and finally result in apoptosis in multiple lines of breast cancer cells [23].

The Food and Drug Administration in 1973 approved the 17α-methyltestosterone (MT) for the treatment of breast cancer [24].

This drug is a synthetic androgen that is utilized broadly as a constituent of hormone substitution therapy with the affinity for the androgen receptor. MT could influence local estrogen formation by regulating aromatase expression or by restraining aromatase activity, the contrary is not aromatized [25].

In this study, we designed a dual drug delivery system for MT anti-cancer drug using HSA NPs to reduce its side effects on the normal cells; DA was used as a targeting moiety as well.

MATERIALS AND METHODS
Materials

MT was purchased from Aburaihan pharmaceutical company. N-hydroxysuccinimide (NHS) and 1-ethyl-3-(3-dimethylaminopropyl)-carbodiimide (EDC) were obtained from Merck Co. (Darmstadt, Germany).
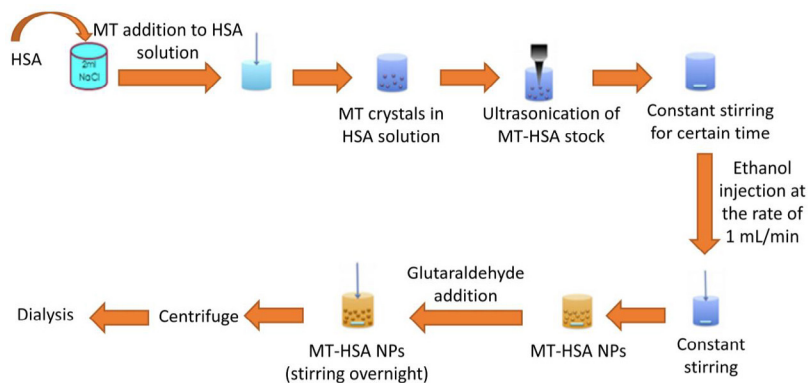

Fig 1. Preparation of MT-HSA NPs using ultrasonication and desolvation methods

HSA (purity 96%–99%), 8% glutaraldehyde, and DA were purchased from Sigma-Aldrich (St. Louis, MO, USA).

Preparation of MT–HSA NPs using ultrasonication

MT-HSA NPs were prepared using ultrasonication in the fabrication procedure (Fig 1) using the desolvation method [26]. First, HSA was dissolved in 2.0 mL of 10 mM NaCl [3, 27]. Second, MT (poorly soluble) was added to HSA solution and ultrasonicated at 20 W for 30 min with a probe-type sonicator [28]. Then, the pH was adjusted to 8 by adding 0.1 M NaOH. The MT-HSA solution was stirred for proper time with a magnetic stirrer (550 rpm) at room temperature to achieve MT adsorption on the HSA complex. Then, NPs were spontaneously created by adding ethanol (dropwise) to the MT-HSA solution with a rate of 1.0 mL/min [3, 29]. To stabilize these NPs, it was needed to add 120 L of 8% glutaraldehyde. The crosslinking of NPs was induced for 24 hours under continual magnetic stirring at room temperature [30]. Finally, the purification of obtained albumin NPs and removing unloaded drug was performed using centrifugation (8,000 g, 30 min) along with the redispersion process in an ultrasonication bath. Finally, NPs were dispersed in phosphate buffered saline (PBS) (0.01 M).

Dopamine conjugation on MT-HAS-NPs

The synthesis of MT-HSA-DA NPs was performed as a modified technique represented by Kim et al., and Lee et al. [31]. 0.3 mg of NHS and 0.5 mg of EDC were dissolved in 1 mL of PBS (pH 6.6, 0.01 M) for 15 minutes at room temperature to prepare activation buffer. The activated buffer was added to MT-HSA-DA NPs dropwise under slow stirring. After 20 min, 0.2 mg of DA was added, and the pH was adjusted to 6.8 using 0.01 M HCl. The solution was incubated for 3 hr. The mixture was dialyzed using dialysis bag of 12 kDa cut-off placed in 0.01 M phosphate buffer (pH 7.4, 450 mL) three times at 2 hr intervals to completely expel unloaded DA molecules from MT-HSA-DA NPs.

Effect of various factors on polydispersity index and size of NPs

In this study, we investigated various parameters such as pH, the rate of addition of ethanol, and albumin concentration that are affecting the polydispersity index (PDI), and the size of NPs [32] and thus Zetasizer (model 3600,

Malvern Instruments Ltd., Worcestershire, UK) was used. For obtaining of zeta-potential, the NPs suspension was centrifuged to remove the excess drug and also phosphate buffer and sediment NPs were separated from the solution, then water with the same volume was added and probe sonicated. One of the factors in each step was variable while the others were fixed and their influences on particle size and PDI were studied. We aimed to survey the affecting factors on particle size and optimize the procedure in such a way to attain the NPs with minimum particle size and PDI. The results of the present study have shown that the size of particles plays a significant role in the absorption of NPs and is an effective factor for cellular uptake many cell lines, only submicron particles can be taken up well instead of the larger size microparticles, which is in agreement with published literature [33].

Characterization of MT-HSA NPs

To investigate the structure of MT-HSA NPs, scanning electron microscopy (SEM; TESCAN, MIRA III model) was carried out at an operating voltage of 15kV. For this purpose, 4-5 drops of NPs were placed on a glass slide to dry at room temperature and subsequently scanned through SEM operating at 25 kV.

Atomic force microscopy (AFM) (MobileS, Nanosurf, Switzerland) was performed to examine the structure of MT-HSA NPs with noncontact mode. A few drops of the sample were deposited on a glass slide and dried at room temperature, subsequently scanned. Transmission electron microscopy was used to inspect and observe the structure and size of the MT-HSA NPs. A few drops of NPs were placed on a carbon film-coated Transmission electron microscopy (TEM) grid and dried at 37 ° C. The device used for sample scanning was the FEI TECNAI G2 model that acted at a 100 kV accelerator voltage. Differential Scanning Calorimetry (DSC) of MT, HSA, and MT-HSA NPs was carried out using DSC (SDT Q 600 V20.9 Build 20). The analysis of samples was performed with a temperature range of 0-200 °C at a rate of 10 °C/ min.

Determination of drug entrapment efficiency and drug loading

The drug loading (DL) and encapsulation efficiency (EE) of MT in MT-HSA NPs were determined using a UV-vis spectrometer. The

Nanomed. J. 8(2): 147-155, Spring 2021

149

concentration of MT in NPs was evaluated using the calibration curve of MT with concentration between 0.09-0.9 mg/mL (y = 1.254 x + 0.009, R2= 0.98) at 241 nm. The calibration curve was obtained from the UV absorbance of several standard MT aqueous solutions. The freshly prepared NPs suspensions were centrifuged at 8000 rpm for 30 min. The supernatants were then removed for the determination of free MT in the suspensions.

Calculation of DL and EE was performed utilizing presented formulas:

$$DL(\%) = \frac{Total\ MT - Free\ MT}{MT - HSA\ NPs\ weight} \times 100 \qquad (1)$$

$$EE(\%) = \frac{Total\ MT - Free\ MT}{Total\ MT} \times 100 \qquad (2)$$

Drug release of MT-HSA NPs

In vitro release study of MT-HSA NPs was done via the dialysis bag diffusion technique. MT-HSA NPs were placed in a dialysis bag (cut off 12 kDa). The dialysis bag was placed in 100 mL of PBS with different pHs (5.5, 6.8, and 7.4), and maintained at room temperature with constant stirring at 550 rpm [34, 35]. At distinct time intervals, a 2 mL aliquot of the release medium was removed and the same volume of fresh buffer was added into the system. The concentration of MT in the release medium was calculated from the MT absorption calibration curves at 241 nm.

In vitro cytotoxicity study

MTT method was used to evaluate proliferation inhibition effects on the cancer cell line, using 8, 16, and 32 μg/mL concentrations of HSA, HSA-DA, MT, HSA-MT, and HSA-MT-D .In the present study, the MCF-7 (ATCC HTB-22TM) - the adherent epithelial adenocarcinomas coming by the mammary glands taken from the metastatic pleural outflow area was applied. Cell line has grown in 75-cm2 tissue culture containers well-kept in Dulbecco's Modified Eagle Medium (DMEM) and 10% heat-inactivated fetal bovine serum, 100 U mL-1 penicillin and 100 μg mL-1 Streptomycin were added. In 2-day intervals, the medium was revived, and cultivated cells were kept warm at 37 °C in a humid setting (95% air and 5% CO2). To achieve proper confluency, these cells were separated into two parts using Trypsin-EDTA (0.25%) solution to test the viability factor. After the adherence, the next step was to drive out the medium and treat the cells using 100 μL of HSA, HSA-DA, HSA-MT, and HSA-MT-DA at concentrations referred to above in culture media. In the first three days of incubation, cell samples were investigated to determine their viability by applying a standard MTT test. 50 μL of MTT (0.5 mg/mL) was supplemented to the medium and well-kept in an incubation setting for 4 h. Then the medium was taken away, and 150 μL of DMSO was added to each sample to dissolve purple formazan crystals. A microplate reader (Lab System Multiskan, Santa Clara, and Ca) at the wavelength of 241 nm was applied to assess the amount of solution absorbed. The formula presented below was used to compute the cell viability percentage of HSA, HSA-DA, MT, HSA-MT, and HSA-MT-DA.

$$Cell\ viability\ (\%) = \frac{OD\ of\ treated\ cells}{OD\ of\ untreated\ cells} \times 100 \qquad (3)$$

RESULTS AND DISCUSSION

The aim of the current study was to design a targeted system of HSA NPs for MT delivery to breast cancer cells.
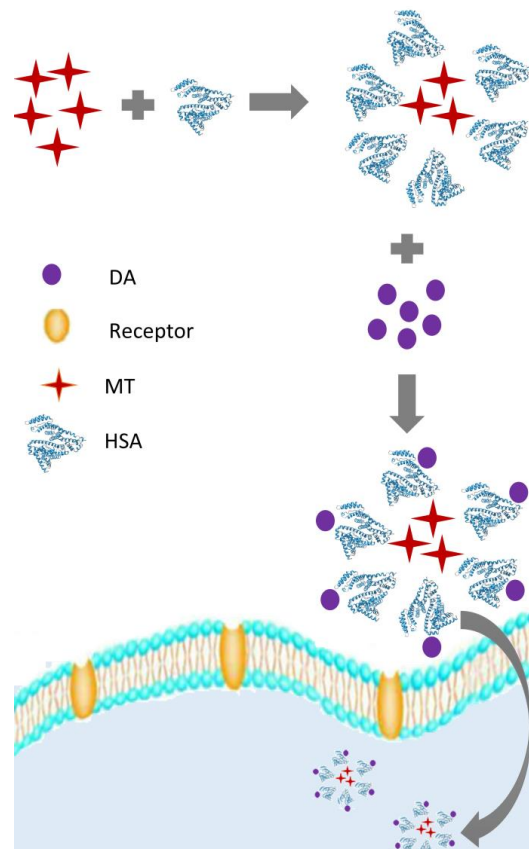
Scheme1. Representation of delivery MT-HSA-DA NPs to cancer cells

150

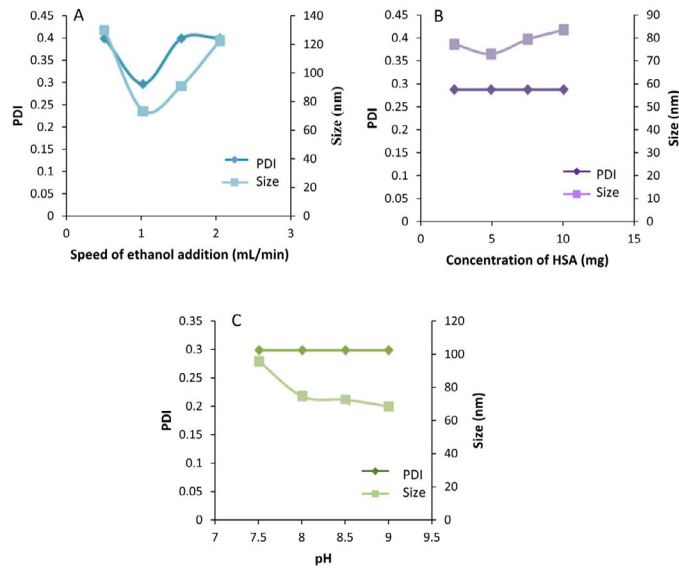*Nanomed. J. 8(2): 147-155, Spring 2021*

Fig 2. (a) Effect of the addition speed of ethanol (b) HSA concentration and (c) pH on PDI and particle size

NPs can increase the solubility of hydrophobic drugs in aqueous solution and can passively accumulate in tumor tissue through the enhanced permeability and retention (EPR) effect using targeting ligands such as human epidermal growth factor, DA, and folic acid [21, 36].

D1R is overexpressed on breast cancer cells and it enables DA to enter the cancer cells via endocytosis (Scheme 1). Modified desolvation was applied as the main method to create HSA NPs containing a high amount of MT. Ultrasonication was applied to increase the EE and DL, moreover, caused to reduce the interactions of the inner particle [3, 37]. HSA will avoid MT aggregate after the elimination of ultrasound because of its surface-active and stabile character [38]. Ethanol was used as a dissolving factor since it functions like an anti-solvent to HSA and it can reduce the amount of solubility of HSA in water and promotes the process of forming NPs through precipitation. Ethanol addition leads to small changes in the native structure of protein [39]. Ethanol has been used as a desolvating factor that acts as an HSA anti-solvent and can facilitate the process of MT-HSA NPs formation; moreover, it can reduce the solubility of HSA in the aqueous phase [39, 40]. After desolvation, cross-linking by glutaraldehyde via reduction of the amino groups on the albumin NPs which leads to hardening the albumin NPs, and also diminishes the stability of the carrier system [10, 11, 37].

The effect of speed of ethanol addition on the particle size and PDI

To understand the effect of speed of ethanol addition on the particle size and PDI, ethanol was added to the albumin solution at different speeds (0.5, 1, 1.5 and 2 mL/min). As indicated in Fig 2a, the early reduction in the particle size was observed with a rise in the speed of ethanol addition from 0.5 mL to 1 mL/min. However, more increase in the speed of addition leads to the larger particle size. This could be due to the fast desolvation procedure that leads to precipitation of albumin and other proteins and more aggregations [32, 41]. So, the speed of adding ethanol should be under control which was kept at 1 mL/min. The results are in agreement with the previous reports [32]. Also, a more uniform particle size distribution was observed at a 1 mL/min addition rate. Since faster addition speed (e.g. 1.5 and 2 mL/min) leads to non-uniform particles because of insufficient time for the complete desolvation [32].

The influence of different HSA concentration on the size and PDI

The influence of different HSA concentration on the size and PDI was investigated similar to other articles [29, 33, 42]. Fig 2b shows that a rise in the concentration of albumin ranging from 2.5-10 mg/mL results in an increase in the size of the NPs. However, 5 mg/mL was the most effective concentration in size. Nevertheless, results show that this factor does not affect the PDI.

Nanomed. J. 8(2): 147-155, Spring 2021

151

The investigation of the pH effect

For the investigation of the pH effect, the pH value of the HSA solution before the desolvation procedure was measured as the major factor determining particle size [42]. Increasing pH has led to a decrease in the size of the NPs, which is in agreement with the literature [33] (Fig. 2c). As indicated, the smallest NPs were obtained at pH 9, however, this factor does not affect PDI. The effect of the pH was investigated between 4-9, because albumin is stable in this range [43].
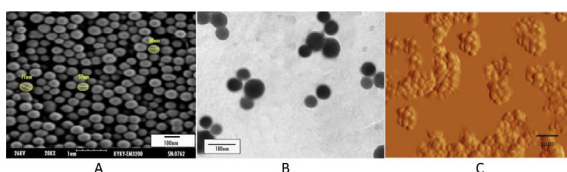

Fig 3. (a) SEM, (b) TEM and (c) AFM images of MT-HSA NPs

Characterization of MT-HSA and MT-HSA-DA NPs

In this study, we investigated the influence of the different factors on the size and PDI of NPs, such as the pH solution, the speed of ethanol addition, and the HSA concentration. Following carrying out optimization, the final process of NPs production was selected. The same particles with small size distribution and PDI were obtained at pH 9, HSA concentration of 5 mg/mL, and the addition rate of 1 mL/min. With the modified desolvation technique reported in the present study, we achieved MT-loaded HSA NPs of diameters between 60-70 nm and PDI of 0.3. The size of MT-HSA NPs was increased from 69 to 82 nm after DA conjugation on the surface of these NPs. Also, the zeta potential of these NPs reduced from -17.28 ± 0.3 to -14.37 ± 2.61 mV due to the DA functionalization of MT-HSA. By the attachment of the DA molecules, unloaded amino groups on the MT-HSA NPs are reduced. Particle size, PDI, and zeta potential for DA functionalized and non-functionalized MT-HSA NPs are shown in Table 1.

Table 1. Physico-chemical characters of MT - HSA NPs and MT-HSA-DA NPs

Sample name	Size (nm)	PDI	Zeta potential (mV)
MT-HSA	69	0.3	-17 ± 1.12
MT-HSA-DA	82	0.3	-14.37 ± 2.61

The morphology of the obtained NPs was analyzed using scanning electron microscopy and transmission electron microscopy. The SEM and TEM images (Fig 3a, b) indicate that NPs shape is smooth and spherical with uniform size distribution in the desirable range of their size. The size of NPs by SEM and TEM is 69 nm and 60 nm respectively. Also, the atomic force microscopy was performed to examine the topography of NPs that shows the smooth surface of the NPs (Fig 3c). NPs are well-suited to the gates which are opening at the cellular and sub-cellular levels since both of them are nanoscaled. The narrowest capillaries are about 2,000 nanometers in diameter; therefore NPs with less than 300 nm are effective for transfer across capillaries. Thus the ability of NPs to enter cells increases with improving their bioavailability to cross capillary walls [44].

The pure MT thermogram at 163.25 ° C showed an endothermic peak that is related to its melting point (Fig 4).
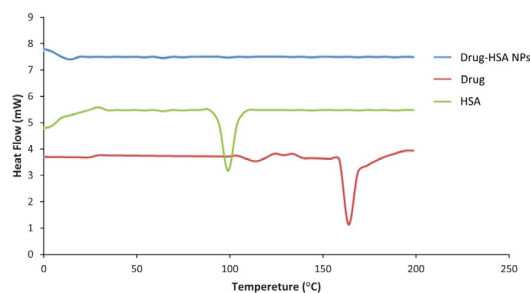

Fig 4. DSC of pure MT, HSA and MT- HSA NPs

The HSA thermocouple peak is also shown at 100 ° C. For NPs, the absence of crystalline MT in calorimetric cure indicates that the drug is present in the amorphous phase and is loaded in the NPs [45-47].

Physical stability of NPs

Changes in the size and zeta potential of NP are defined for the physical stability of NPs [46]. Stability studies of MT-HSA NPs were carried out. The sizes of particles were measured to estimate their stability. Measuring of the physiochemical characteristic of NPs has been done through DLS after a 6-month-term of storage. The samples were stored at 4° C for six months. The sizes of particles were increased to 80-85 nm, while particles were stable as well.

In vitro drug release studies

Small particles have large surface areas, which allow the drugs to be localized near the particle surface that subsequently results in faster drug release. Large particles have large cores in which

the drugs are encapsulated easily and slowly diffuse out [39]. In this study, drug release from NPs with a size of 69 nm is considered. The release profiles of MT loaded HSA in PBS at three different pHs are shown in Fig 5. The results show that the drug release after 80 h, at pH values of 5.5, 6.8, and 7.4 are close to 89%, 78% and 69%, respectively, that demonstrate higher acidity cause to higher drug release from HSA NPs. Thus, one can conclude that release behavior is depended on the pH value.
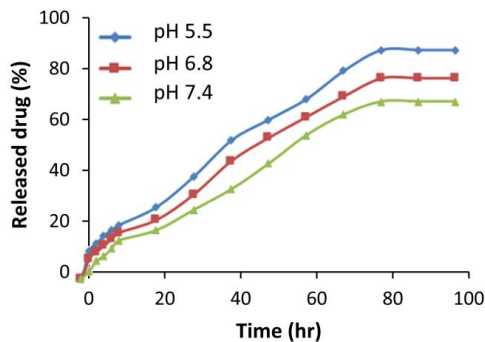

Fig 5. Percentages of the release of MT from MT - HSA NPs at pH 5.5, 6.8, and 7.4

The drug entrapment efficiency and drug loading

The drug entrapment efficiency and drug loading are two characteristics of NPs. Several factors such as the natures of encapsulated molecules and NPs, and the type of drug loading method affect the DL and EE. In our study, EE was calculated using UV-Vis spectroscopy. The amount of MT present in the supernatant was determined using a calibration curve at 241 nm. Then, after drawing of the calibration curve, DL and EE were calculated according to the MT calibration curve, their equations and the amounts of MT loaded HSA NPs weight. Results showed about 91% EE for MT in MT loaded HSA NPs and DL was 14%.

In vitro cytotoxicity assay

The amount of MTT depends on the division of soluble yellow tetrazolium rings and the emergence of insoluble purple formazan crystals through the mitochondrial enzyme in alive cells. Therefore, the number of alive cells has a direct effect on formazan formation. The toxicity of HSA, HSA-DA, MT, HSA-MT, and HSA- MT-DA in the MCF-7 cell line is presented in Fig 6 after 24 h. According to Fig 6 MT does not affect cancer cells significantly but MT loaded HSA NPs and MT-HSA-DA NPs kill the breast cancer cells more efficient

than MT alone. It probably is due to higher uptake of nanocarrier via HSA and DA receptors on the cell surface and it can be mentioned that entering of nanocarrier to the cells is improved by DA as a targeting molecule on its surface [21] and the presence of GP60 receptor of HSA on cancer cells [13]. MTT test revealed that 32 µg/mL of free MT, MT loaded HSA, and HSA-MT-DA lowers the cell growth to 23.66 ± 1.52, 23.33 ± 3.5, and 8.66 ± 0.45 (%), respectively and HSA, and HSA-DA were not toxic to breast cancer cell line.
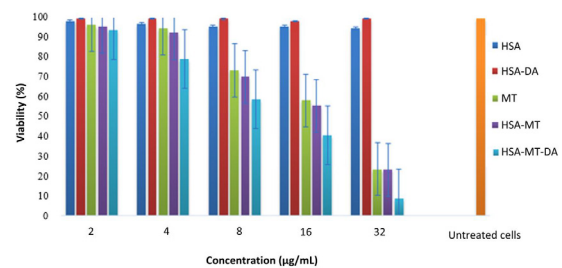

Fig 6. The effect of HSA, HSA–FA, MT, HSA–MT, and HSA–MT–DA concentrations on the viability of MCF-7 cell line after 24 h

CONCLUSION

In our study, by the modified desolvation method, DA targeted HSA–MT conjugated NPs were synthesized as a desirable targeted drug delivery system to encapsulate MT, improve therapeutic effects of MT, and decrease its complication effects. Encapsulation of MT into HSA NPs led to the enhancement of its solubility and stability. MT-HSA- DA NPs with size less than 100 nm were produced using the optimized process. Due to overexpression of DA receptors, DA targeted MT-HSA NPs could be taken up by the cancerous cells. Also, MTT assay with free MT, MT loaded HSA and HSA-MT-DA showed diminishes in the cell viability after 24 h. It is considered that the dual-targeted drug delivery system designed in the present study could improve the efficiency of drug and decreases its undesirable side effects.

REFERENCES

1. Senapati S, Mahanta AK, Kumar S, Maiti P. Controlled drug delivery vehicles for cancer treatment and their performance. Signal transduction and targeted therapy. Signal transduct target ther. 2018; 3 (1): 7.

2. Norouzi P, amini M, Mottaghitalab F, Mirzazadeh Tekie FS, Dinarvand R, Mirzaie ZH, Atyabi F. Design and fabrication of dual-targeted delivery system based on gemcitabine conjugated human serum albumin nanoparticles. Chem Biol Drug Des. 2017.

3. Kouchakzadeh H, Shojaosadati SA, Shokri F. Efficient loading and entrapment of tamoxifen in human serum albumin

Nanomed. J. 8(2): 147-155, Spring 2021

153

based nanoparticulate delivery system by a modified desolvation technique. Chem Eng Res Des. 2014; 92 (9): 1681-1692.

4.Chida T, Miura Y, Cabral H, Nomoto T, Kataoka K, Nishiyama N. Epirubicin-loaded polymeric micelles effectively treat axillary lymph nodes metastasis of breast cancer through selective accumulation and pH-triggered drug release. J Control Release. 2018; 292: 130-140.

5.Zununi Vahed S, Salehi R, Davaran S, Sharifi S. Corrigendum to" Liposome-based drug co-delivery systems in cancer cells" (Mater. Sci. Eng.(2017) C 71 (1327-1341) (S0928493116322871)(10.1016/j. msec. 2016.11. 073)). Mater Sci Eng C. 2018; 83: 247.

6.Xiong Z, Shen M, Shi X. Dendrimer-based strategies for cancer therapy: Recent advances and future perspectives. Sci China Mater. 2018; 61(11): 1387-1403.

7.Lim E-K, Chung BH, Chung SJ. Recent advances in pH-sensitive polymeric nanoparticles for smart drug delivery in cancer therapy. Curr Drug Targets. 2018; 19(4): 300-317.

8.Yu X, Trase I, Ren M, Duval K, Guo X, Chen Z. Design of nanoparticle-based carriers for targeted drug delivery. J Nanomater. 2016; 2016.

9.Elzoghby AO, Samy WM, Elgindy NA. Protein-based nanocarriers as promising drug and gene delivery systems. J Control Release. 2012; 161(1): 38-49.

10.Zorzi A, Linciano S, Angelini A. Non-covalent albumin-binding ligands for extending the circulating half-life of small biotherapeutics. Medchemcomm. 2019.

11.Dockal M, Carter DC, Rüker F. The three recombinant domains of human serum albumin structural characterization and ligand binding properties. J Biol Chem. 1999; 274(41): 29303-29310.

12.Karimi M, Bahrami S, Ravari SB, Zangabad PS, Mirshekari H, Bozorgomid M, Shahreza S, Sori M, Hamblin MR. Albumin nanostructures as advanced drug delivery systems. Expert Opin Drug Deliv. 2016; 13(11): 1609-1623.

13.Lomis N, Westfall S, Farahdel L, Malhotra M, Shum-Tim D, Prakash S. Human serum albumin nanoparticles for use in cancer drug delivery: process optimization and in vitro characterization. Nanomaterials. 2016; 6(6): 116.

14.Niknejad H, Mahmoudzadeh R. Comparison of different crosslinking methods for preparation of docetaxel-loaded albumin nanoparticles. Iran J Pharm Res. 2015; 14 (2): 385.

15.Taneja N, Singh KK. Rational design of polysorbate 80 stabilized human serum albumin nanoparticles tailored for high drug loading and entrapment of irinotecan. Int J Pharm. 2018; 536(1): 82-94.

16.Kratz F. Albumin as a drug carrier: design of prodrugs, drug conjugates and nanoparticles. J Control Release. 2008; 132(3): 171-183.

17.Zhao S, Wang W, Huang Y, Fu Y, Cheng Y. Paclitaxel loaded human serum albumin nanoparticles stabilized with intermolecular disulfide bonds. Medchemcomm. 2014; 5(11): 1658-1663.

18.Saleh T, Soudi T, Shojaosadati SA. Redox responsive curcumin-loaded human serum albumin nanoparticles: Preparation, characterization and in vitro evaluation. Int J Biol Macromol. 2018; 114: 759-766.

19.Nateghian N, Goodarzi N, Amini M, Atyabi F, Khorramizadeh MR, Dinarvand R. Biotin/folate-decorated human serum albumin nanoparticles of docetaxel: comparison of chemically conjugated nanostructures and physically loaded nanoparticles for targeting of breast cancer. Chem

Biol Drug Des. 2016; 87(1): 69-82.

20.Kouchakzadeh H, Hoseini Makarem S, Shojaosadati S. Simultaneous loading of 5-florouracil and SPIONs in HSA nanoparticles: Optimization of preparation, characterization and in vitro drug release study. Nanomed J. 2016; 3(1): 35-42.

21.Masoudipour E, Kashanian S, Maleki N. A targeted drug delivery system based on dopamine functionalized nano graphene oxide. Chem Phys Lett. 2017; 668: 56-63.

22.Das P, Jana NR. Dopamine functionalized polymeric nanoparticle for targeted drug delivery. RSC Adv. 2015; 5(42): 33586-33594.

23.Borcherding DC, Tong W, Hugo ER, Barnard DF, Fox S, LaSance K, Shaughnessy E, Ben-Jonathan N. Expression and therapeutic targeting of dopamine receptor-1 (D1R) in breast cancer. Oncogene. 2016; 35(24): 3103.

24.Sun J, Wei Q, Zhou Y, Wang J, Liu Q, Xu H. A systematic analysis of FDA-approved anticancer drugs. BMC Syst Biol. 2017; 11(5): 87.

25.Mor G, Eliza M, Song J, Wiita B, Chen S, Naftolin F. 17α-Methyl testosterone is a competitive inhibitor of aromatase activity in Jar choriocarcinoma cells and macrophage-like THP-1 cells in culture. J Steroid Biochem Mol Biol. 2001; 79(1-5): 239-246.

26.Kamali M, Dinarvand R, Maleki H, Arzani H, Mahdaviani P, Nekounam H, Adabi M, Khosravani M. Preparation of imatinib base loaded human serum albumin for application in the treatment of glioblastoma. RSC Adv. 2015; 5(76): 62214-62219.

27.Jahanban-Esfahlan A, Dastmalchi S, Davaran S. A simple improved desolvation method for the rapid preparation of albumin nanoparticles. Int J Biol Macromol. 2016; 91: 703-709.

28.Agarwal A, Lvov Y, Sawant R, Torchilin V. Stable nanocolloids of poorly soluble drugs with high drug content prepared using the combination of sonication and layer-by-layer technology. J Control Release. 2008; 128(3) 255-260.

29.Kimura K, Yamasaki K, Nakamura H, Haratake M, Taguchi K, Otagiri M. Preparation and in vitro analysis of human serum albumin nanoparticles loaded with anthracycline derivatives. Chem Pharm Bull. 2018; 66(4): 382390-.

30.Sebak S, Mirzaei M, Malhotra M, Kulamarva A, Prakash S. Human serum albumin nanoparticles as an efficient noscapine drug delivery system for potential use in breast cancer: preparation and in vitro analysis. International journal of nanomedicine Int J Nanomedicine.2010; 525: 5.

31.Kim S, Jang Y, Jang LK, Sunwoo SH, Kim T-i, Cho S-W, Lee JY. Electrochemical deposition of dopamine–hyaluronic acid conjugates for anti-biofouling bioelectrodes. J Mater Chem B. 2017; 5(23): 4507-4513.

32.Taneja N. Preparation of size controlled albumin nanoparticles and its in- vitro safety evaluation. Eur J Pharm Med Res. 2017; 4 (07): 478-484.

33.Mehravar R, Jahanshahi M, Saghatoleslami N. Human serum albumin (HSA) nanoparticles as drug delivery system: preparation, optimization and characterization study. Dyn Biochem Process Biotechnol Mol Biol. 2009; 3: 51-56.

34.Guo H, Fei S, Zhang Y, Zhang Y, Gou J, Zhang L, He H, Yin T, Wang Y, Tang X. Teniposide-loaded multilayer modified albumin nanoparticles with increased passive delivery to the lung. RSC Adv. 2016; 6 (84): 81110-81119.

35.Tao X, Jin S, Wu D, Ling K, Yuan L, Lin P, Xie Y, Yang X. Effects of particle hydrophobicity, surface charge, media

154

Nanomed. J. 8(2): 147-155, Spring 2021

pH value and complexation with human serum albumin on drug release behavior of mitoxantrone-loaded pullulan nanoparticles. Nanomaterials. 2016; 6 (1): 2.

36. Sun Y, Zhao Y, Teng S, Hao F, Zhang H, Meng F, Zhao X, Zheng X, Bi Y, Yao Y. Folic acid receptor-targeted human serum albumin nanoparticle formulation of cabazitaxel for tumor therapy. Int J Nanomedicine. 2019; 14: 135.

37. Keum C-G, Noh Y-W, Baek J-S, Lim J-H, Hwang C-J, Na Y-G, Shin S-C, Cho C-W. Practical preparation procedures for docetaxel-loaded nanoparticles using polylactic acid-co-glycolic acid. Int J Nanomedicine. 2011; 6: 2225.

38. Hawe A, Friess W. Stabilization of a hydrophobic recombinant cytokine by human serum albumin. J Pharm Sci. 2007; 96 (11): 2987-2999.

39. Ghosh P, Roy AS, Chaudhury S, Jana SK, Chaudhury K, Dasgupta S. Preparation of albumin based nanoparticles for delivery of fisetin and evaluation of its cytotoxic activity. Int J Biol Macromol. 2016; 86: 408-417.

40. Mohammad-Beigi H, Shojaosadati SA, Morshedi D, Mirzazadeh N, Arpanaei A. The effects of organic solvents on the physicochemical properties of human serum albumin nanoparticles. Iran J Biotechnol. 2016; 14 (1): 45.

41. Ahsan SM, Rao CM. The role of surface charge in the desolvation process of gelatin: implications in nanoparticle synthesis and modulation of drug release. Int J Nanomedicine. 2017; 12: 795.

42. Langer K, Balthasar S, Vogel V, Dinauer N, Von Briesen H, Schubert D. Optimization of the preparation process for human serum albumin (HSA) nanoparticles. Int. J. Pharm. 2003; 257 (1-2): 169-180.

43. Choi J-S, Meghani N. Impact of surface modification in BSA nanoparticles for uptake in cancer cells. Colloids Surf B Biointerfaces. 2016; 145: 653-661.

44. Sivasankar M, Kumar BP. Role of nanoparticles in drug delivery system. Int. J. Pharm. Biomed. Res. 2010; 1 (2): 41-66.

45. Qu N, Sun Y, Li Y, Hao F, Qiu P, Teng L, Xie J, Gao Y. Docetaxel-loaded human serum albumin (HSA) nanoparticles: synthesis, characterization, and evaluation. Biomedical engineering online. Biomed. Eng. Online. 2019; 18 (1): 11.

46. Boateng-Marfo Y, Dong Y, Loh ZH, Lin H, Ng WK. Intravenous human serum albumin (HSA)-bound artemether nanoparticles for treatment of severe malaria. Colloids Surf. A Physicochem. Eng. Asp. 2018; 536: 20-29.

47. Yewale C, Baradia D, Patil S, Bhatt P, Amrutiya J, Gandhi R, Kore G, Misra A. Docetaxel loaded immunonanoparticles delivery in EGFR overexpressed breast carcinoma cells. J Drug Deliv Sci Technol. 2018; 45: 334-345.

Nanomed. J. 8(2): 147-155, Spring 2021

155